INSTITUTE OF PHYSICS PUBLISHING JOURNAL OF GEOPHYSICS AND ENGINEERING
J. Geophys. Eng. **3** (2006) 271–282 doi:10.1088/1742-2132/3/3/009

The application of two-parameter velocity and slowness functions in approximating seismic reflection travel times

Xiucheng Wei[1,2], David Booth[2], Yang Liu[3] and Xiang-Yang Li[2]

[1] Petroleum Exploration and Production Research Institute, Sinopec, Xueyuan Road, Beijing 100083, People's Republic of China
[2] Edinburgh Anisotropy Project, British Geological Survey, Edinburgh EH9 3LA, UK
[3] Faculty of Resources and Information, China Petroleum University, Beijing 102249, People's Republic of China

E-mail: weixc@pepris.com and wei_xiucheng@hotmail.com

Received 20 June 2006
Accepted for publication 24 July 2006
Published 17 August 2006
Online at stacks.iop.org/JGE/3/271

Abstract

Seismic reflection travel time–offset curves are complicated, and depend on many parameters. There is a need for simplified equations involving a reduced number of parameters that can be estimated from data and used for moveout correction and a simplified velocity model of the Earth. Many authors have derived explicit equations for travel time as a function of offset, involving several parameters which depend on velocity. Some authors have applied the approach in which velocity varies with offset (velocity with high-order terms or anisotropic properties). Here we present a new approach in which we employ velocity variation with depth instead of offset. A simple linear variation of velocity is used to derive expressions for travel time and offset as a function of ray parameter, from which the variation of travel time with offset can be obtained. Only two parameters are involved in defining the velocity–depth profile, but the resulting travel time–offset curves are good approximations. Two-parameter linear variations of slowness with depth, and velocity and slowness with depth and zero-offset travel time, have also been derived and the relationships between them are described. Comparison of the new approximations with those of Taner and Koehler (1969 *Geophysics* **34** 859–81), and the large-offset approximations of Causse *et al* (2000 *Geophys. Prospect.* **48** 763–78) was performed using 1D plane-layered models with different velocity profiles. Taner and Koehler and Causse *et al* approximations are inaccurate for large and small offsets respectively, while the new approximations show improved accuracy and can be applied over the whole range of offsets. The velocity and slowness expressions can also be used for moveout correction. Synthetic and real records are used to demonstrate their effectiveness.

Keywords: velocity, slowness, travel time

(Some figures in this article are in colour only in the electronic version)

Introduction

The hyperbolic approximation for reflection travel times (Dix 1955) is generally used for velocity analysis and stacking. In most cases this approximation is accurate at small offset-to-depth ratio only, and many authors have proposed improvements to it. Taner and Koehler (1969) extended the approximation by deriving a higher order series applicable to isotropic layered media for CMP gather:

$$t^2(y) = d_0 + d_2y^2 + d_4y^4 + d_6y^6 + d_8y^8 + \cdots, \qquad (1)$$

where y represents the offset. Several authors (Al-Chalabi 1973, 1974, May and Straley 1979, Gidlow and Fatti 1990,

Kaila and Sain 1994, Thore *et al* 1994) have shown that it is possible to improve velocity analysis and stacking by using more than two terms of this series. Reflection travel times are non-hyperbolic even for a single homogeneous layer if anisotropy is present, and it is common to use (1) with three terms (Hake *et al* 1984) or a modified three-term approximation with higher accuracy and stability at large offsets (Tsvankin and Thomsen 1994). All these approximations are generally applicable only to relatively small offset-to-depth ratios.

To obtain a travel time approximation with good accuracy at large offsets, Causse *et al* (2000) derived a series based on a large-offset approximation:

$$t^2(y) = c_1 y + c_0 + \frac{c_{-1}}{y} + \frac{c_{-2}}{y^2} + \frac{c_{-3}}{y^3} + \frac{c_{-4}}{y^4} + \cdots. \tag{2}$$

The large-offset approximation is most accurate where there is strong ray bending, while the classical small-offset approximation is most accurate in situations of weak ray bending. So, an approximate expression for travel time at all offsets cannot be obtained from any one of these series above.

To avoid the drawbacks of using equations (1) and (2), Causse (2004) derived new approximate travel time equations that do not need any assumption for the offset. The approach is to build approximations that focus on accurately describing the subspace of all realistic reflection travel time curves, formed from the larger space of offset functions represented by equations (1) and (2). The type of the approximations is as follows:

$$t^{\alpha}(y) = c_1 f_1(y) + c_2 f_2(y) + c_3 f_3(y) + \cdots. \tag{3}$$

Equations (1) and (2) represent particular forms of this expression, with exponent α equal to 2 and 1, respectively, and with functions $f_i(y)$ equal to positive and negative integer powers of offset. A set of reference travel time curves are created from a number of realistic velocity models. Causse (2004) described a method to obtain an optimal basis of functions from these reference curves by singular value decomposition, and he shows that equation (3) provides more accurate approximations of the exact travel time curves at all offsets.

Another way to approximate travel time is to use a function of velocity with depth. A common approach is to represent the velocity as a linear function of depth. The function can be called the two-parameter function, because there are two independent parameters (initial velocity and its gradient). Causse and Sénéchal (2006) applied the model-based approach to build accurate travel time approximations into velocity analysis of GPR field data for vertical velocity heterogeneous media.

In this paper, we extend the calculation of the two-parameter velocity function of depth to a velocity function in terms of the vertical travel time t_0. We also present functions of slowness dependent on depth and vertical travel time t_0. Since the functions have only two parameters, they are much simpler than equation (3). To demonstrate the improved accuracy and applicability of the two-parameter velocity and slowness functions over a wide range of offsets, we apply our approximations, and those given by equations (1) and (2), to different simple plane-layered models, and discuss the performance of each. Finally, we use synthetic and real records to show that the two-parameter velocity and the slowness method also give accurate moveout corrections over a wide range of offsets, and we draw some conclusions on its functionality.

Two-parameter functions for velocity and slowness

Considering a seismic wave travelling through a stack of plane homogeneous isotropic layers, its ray path from source to receivers can be decomposed into ray segments numbered from 1 to N. The velocity associated with ray segment i is denoted by V_i. This may represent either the P- or S-wave velocity, depending on the wave mode. The corresponding slowness $(1/V_i)$ is represented by S_i. Denoting the corresponding layer thickness by Δz_i and using the ray parameter p, the travel time t and offset y can be expressed as

$$t = \sum_i \frac{1}{\sqrt{1 - p^2 V_i^2}} \frac{\Delta z_i}{V_i}, \tag{4}$$

and

$$y = \sum_i \frac{p V_i}{\sqrt{1 - p^2 V_i^2}} \Delta z_i. \tag{5}$$

When using the equivalent continuous velocity or slowness model instead of a layered model, equations (4) and (5) can be written as

$$t = \int_z \frac{1}{\sqrt{1 - p^2 V_z^2}} \frac{\mathrm{d}z}{V_z}, \tag{6}$$

and

$$y = \int_z \frac{p V_z}{\sqrt{1 - p^2 V_z^2}} \mathrm{d}z. \tag{7}$$

Velocity with depth

The typical linear function of velocity with depth can be described as

$$V_z = V_0 + kz, \tag{8}$$

where V_z is the velocity at depth z, parameter V_0 is the initial velocity at depth $z = 0$ (intercept) and k is the gradient (the rate of variation of velocity with depth). We have

$$\frac{\mathrm{d}V_z}{\mathrm{d}z} = k, \tag{9}$$

$$t = \int_z \frac{1}{\sqrt{1 - p^2 V_z^2}} \frac{\mathrm{d}z}{V_z} = \frac{1}{kp} \int_{V_z} \frac{1}{\sqrt{\frac{1}{p^2} - V_z^2}} \frac{\mathrm{d}V_z}{V_z} \tag{10}$$

and

$$y = \int_z \frac{p V_z}{\sqrt{1 - p^2 V_z^2}} \mathrm{d}z = \frac{1}{k} \int_{V_z} \frac{V_z}{\sqrt{\frac{1}{p^2} - V_z^2}} \mathrm{d}V_z. \tag{11}$$

So the solution of equations (10) and (11) becomes

$$t = -\frac{1}{k}\ln\frac{1+\sqrt{1-p^2V_z^2}}{pV_z}\Bigg|_{V_0}^{V_{z_r}}, \tag{12}$$

$$y = -\frac{1}{kp}\sqrt{1-p^2V_z^2}\Bigg|_{V_0}^{V_{z_r}}, \tag{13}$$

where z_r and V_{z_r} denote the depth of reflector and wave velocity respectively at the depth z_r.

When the ray path is vertical, $p = 0, x = 0$ and

$$t_0 = \frac{1}{k}\ln\frac{V_z}{V_0} = \frac{1}{k}\ln\frac{V_{t_0}}{V_0}, \qquad V_{t_0} = V_0\exp(kt_0). \tag{14}$$

Equations (8) and (14) are equivalent. From (14), we know that velocity can also be described as a function of vertical travel time t_0. It follows that we can extend the equivalent function concept to expressing velocity as a function of travel time t_0 and slowness as a function of depth and vertical travel time t_0.

Velocity with vertical travel time

If velocity is described as

$$V_{t_0} = V_0 + \gamma t_0, \tag{15}$$

$$\frac{\mathrm{d}V_{t_0}}{\mathrm{d}t_0} = \gamma. \tag{16}$$

Then we can obtain

$$t = \int_z \frac{1}{\sqrt{1-p^2V_z^2}}\frac{\mathrm{d}z}{V_z} = \int_{t_0}\frac{1}{\sqrt{1-p^2V_{t_0}^2}}\mathrm{d}t_0 = \frac{1}{\gamma p}\int_{V_{t_0}}\frac{1}{\sqrt{\frac{1}{p^2}-V_{t_0}^2}}\mathrm{d}V_{t_0}, \tag{17}$$

and

$$y = \int_z \frac{pV_z}{\sqrt{1-p^2V_z^2}}\mathrm{d}z = \int_{t_0}\frac{V_{t_0}^2}{\sqrt{\frac{1}{p^2}-V_{t_0}^2}}\mathrm{d}t_0 = \frac{1}{\gamma}\int_{V_{t_0}}\frac{V_{t_0}^2}{\sqrt{\frac{1}{p^2}-V_{t_0}^2}}\mathrm{d}V_{t_0}, \tag{18}$$

the solution of equations (17) and (18) becomes

$$t = \frac{1}{\gamma p}\arcsin pV_{t_0}\Big|_{V_0}^{V_{T_0}}, \tag{19}$$

and

$$y = \frac{1}{\gamma}\left(-\frac{V_{t_0}}{2}\sqrt{\frac{1}{p^2}-V_{t_0}^2}+\frac{1}{2p^2}\arcsin pV_{t_0}\right)\Bigg|_{V_0}^{V_{T_0}}, \tag{20}$$

where t_0 represents the one-way vertical travel time from the surface to the reflector.

Slowness with depth

Describing seismic slowness as

$$S_z = S_0 + \alpha z, \tag{21}$$

so that

$$\frac{\mathrm{d}S_z}{\mathrm{d}z} = \alpha, \tag{22}$$

we have

$$t = \int_z \frac{1}{\sqrt{1-p^2V_z^2}}\frac{\mathrm{d}z}{V_z} = \int_z \frac{S_z^2}{\sqrt{S_z^2-p^2}}\mathrm{d}z = \frac{1}{\alpha}\int_{S_z}\frac{S_z^2}{\sqrt{S_z^2-p^2}}\mathrm{d}S_z, \tag{23}$$

and

$$y = \int_z \frac{pV_z}{\sqrt{1-p^2V_z^2}}\mathrm{d}z = \int_z \frac{p}{\sqrt{S_z^2-p^2}}\mathrm{d}z = \frac{1}{\alpha}\int_{S_z}\frac{p}{\sqrt{S_z^2-p^2}}\mathrm{d}S_z. \tag{24}$$

The solution of equations (23) and (24) becomes

$$t = \frac{1}{\alpha}\left[\frac{S_z}{2}\sqrt{S_z^2-p^2}+\frac{p^2}{2}\ln\left(S_z+\sqrt{S_z^2-p^2}\right)\right]\Bigg|_{S_0}^{S_{z_r}}, \tag{25}$$

and

$$y = \frac{p}{\alpha}\ln\left(S_z+\sqrt{S_z^2-p^2}\right)\Big|_{S_0}^{S_{z_r}}, \tag{26}$$

where z_r and S_{z_r} are used to denote the reflector depth and wave slowness at that depth, respectively.

When the ray path is vertical, $p = 0, x = 0$ and

$$t_0 = \frac{1}{\alpha}\frac{S_z^2}{2}\Big|_{S_0}^{S_z} = \frac{1}{2\alpha}\left(S_z^2-S_0^2\right) = S_0z+\frac{1}{2}\alpha z^2, \qquad S_z = S_{t_0} = \sqrt{2\alpha t_0+S_0^2}. \tag{27}$$

Equations (21) and (27) are equivalent.

Slowness with vertical travel time

Given the slowness equation

$$S_{t_0} = S_0 + \beta t_0, \tag{28}$$

$$\frac{\mathrm{d}S_{t_0}}{\mathrm{d}t_0} = \beta, \tag{29}$$

and equations (23) and (24) can be written as

$$t = \int_z \frac{1}{\sqrt{1-p^2V_z^2}}\frac{\mathrm{d}z}{V_z} = \int_{t_0}\frac{S_{t_0}}{\sqrt{S_{t_0}^2-p^2}}\mathrm{d}t_0 = \frac{1}{\beta}\int_{S_{t_0}}\frac{S_{t_0}}{\sqrt{S_{t_0}^2-p^2}}\mathrm{d}S_{t_0}, \tag{30}$$

and

$$y = \int_z \frac{pV_z}{\sqrt{1-p^2V_z^2}}\mathrm{d}z = \int_{t_0}\frac{p}{S_{t_0}\sqrt{S_{t_0}^2-p^2}}\mathrm{d}t_0 = \frac{p}{\beta}\int_{S_{t_0}}\frac{1}{S_{t_0}\sqrt{S_{t_0}^2-p^2}}\mathrm{d}S_{t_0}, \tag{31}$$

the solution of equations (30) and (31) becomes

$$t = \frac{1}{\beta}\int_{S_{t_0}}\frac{S_{t_0}}{\sqrt{S_{t_0}^2-p^2}}\mathrm{d}S_{t_0} = \frac{1}{\beta}\sqrt{S_{t_0}^2-p^2}\Big|_{S_0}^{S_{T_0}}, \tag{32}$$

and

$$y = \frac{p}{\beta}\int_{S_{t_0}}\frac{1}{S_{t_0}\sqrt{S_{t_0}^2-p^2}}\mathrm{d}S_{t_0} = \frac{1}{\beta}\arccos\frac{p}{S_{t_0}}\Big|_{S_0}^{S_{T_0}}. \tag{33}$$

Table 1. Layer depth, thickness and interval velocities for the models with small velocity variations (A), with larger velocity variations (B) and with a high-velocity layer (C).

Depth (m)	Δz (m)	V^A (m s^{-1})	V^B (m s^{-1})	V^C (m s^{-1})
250	250	1500	1500	1500
650	400	1800	2000	1800
1250	600	1900	2400	1900
1450	200	2000	2800	4600
1950	500	2100	3200	2100
2500	550	2200	3600	2200

Numerical examples

We now compare the accuracy of the functions derived above with those series used by Causse *et al* (2000) and Taner and Koehler (1969), which we shall henceforth refer to as the Causse and T and K series, respectively. We use the same models as Causse *et al* (2000), and calculate the approximate travel times for P-waves reflected at the bottom of three different plane-layer models (A–C) with a reflector depth of 2500 m (table 1).

Given the ratio of offset to depth, the parameters (initial velocity and/or slowness and their gradients) in velocity or slowness functions can be obtained for known models. The relative offset X can be obtained from the layered velocity model. Reflection travel time T can be calculated from equations (4) and (5). Then using the offset X and reflection travel time T in equations (12) and (13), the parameters for velocity variation with depth can be obtained. The same applies to the slowness variation with depth, and the velocity and slowness variation with vertical travel time.

For calculating analytical parameters, the depth of reflector and vertical travel time can be the control parameters for a given layered model. Using the maximum velocity and minimum slowness in the layered model, we have

$$k \in \text{Root}\{f(k) = V_m - (V_m - kz_m)\exp(kt_{0m}) = 0\}, \quad \left(0 < k < \frac{V_m}{z_m}\right) \tag{34}$$

$$\gamma = \frac{2(V_m t_{0m} - z_m)}{t_{0m}^2}, \qquad \left(\gamma < \frac{V_m}{t_{0m}}\right) \tag{35}$$

$$\alpha = \frac{2(S_m z_m - t_{0m})}{z_m^2}, \tag{36}$$

$$\beta \in \text{Root}\{f(\beta) = S_m - (S_m - \beta t_{0m})\exp(\beta z_m) = 0\}, \quad (\beta < 0) \tag{37}$$

where z_m, V_m, S_m and t_{0m} are the maximum depth of the layer being calculated, maximum velocity, minimum slowness and vertical travel time from the surface to the layer, respectively.

The analytical parameters can be used to analyse which function is the best fit for the given layered velocity model. Table 3 shows the RMS errors for models in table 1. The velocity variation with vertical time matches models A and B but the slowness variation with depth matches model C. Though the best results for a given model cannot be obtained from (34) to (37), as the parameters must be adjusted to get best-fit travel times, the RMS errors can help to decide which approximation is the best fit for a given model (table 3).

Table 2. Layer depth, thickness and interval velocities for a model with two high-velocity layers.

Depth (m)	Δz (m)	V (m s^{-1})
300	300	1500
1100	800	2000
1300	200	4599
1900	600	2200
2100	200	4600
3000	900	2400

Table 3. RMS errors from using equations (34)–(37) for models in table 1.

Model	V_z	V_{t_0}	S_z	S_{t_0}
V^A	0.1339	0.1241	0.1509	0.1417
V^B	0.3123	0.2520	0.4734	0.3741
V^C	1.5068	1.7229	0.8298	0.9604

Figure 1 shows the rays for offsets 4, 8 and 12 km in the different models. Since equations (4) and (5) are sums, and the order of the terms in the sum does not play any role in the final result, we can change the layer order to increasing order in velocity from the surface to the reflector in order to more easily determine the two parameters in the linear velocity and/or slowness function. Taking model C of table 1 as example, we can move the high-velocity layer from the middle to the bottom of the layer sequence. Figures 2–4 show the representation of velocity and slowness for the small velocity variations model (A), large velocity variations model (B) and high-velocity layer model (C) respectively.

Figure 5 shows the Taner and Koehler near-offset approximation travel times and Causse large-offset approximation travel times. Figure 6 shows travel times calculated by two-parameter velocity and slowness as illustrated in figures 2–4. Figure 7 shows the approximation errors resulting from the use of Taner and Koehler and Causse approximations for the three models. Figure 8 shows the approximation errors of two-parameter velocity and slowness with depth or vertical travel times. Figure 9 shows the residuals of travel times for the models in table 1. We used offset-to-depth ratios of 1, 3 and 5 to obtain parameters of velocity and slowness. It is seen that the velocity variation with vertical time (green curves in figure 9) is suitable for model B, and slowness variation with depth (yellow curves in figure 9) is the best match for model C. All four functions can be used for model A, corresponding to small velocity variations.

Discussion

We now compare the results obtained using the different approximations, and discuss the performance of the two-parameter functions for velocity and slowness when applied to different velocity depth profiles. Then after setting out the relationships between the functions, we shall use an example to illustrate how velocity and slowness functions of vertical travel time are convenient for velocity analysis and the determination of NMO corrections.

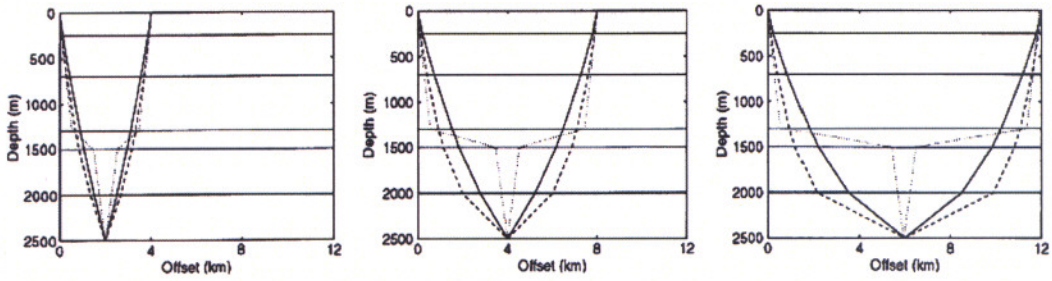

Figure 1. Ray paths for different offsets. The solid, dashed and dotted lines correspond to models (in table 1) with small velocity variations, large velocity variations and a high-velocity layer, respectively (after Causse *et al* 2000).

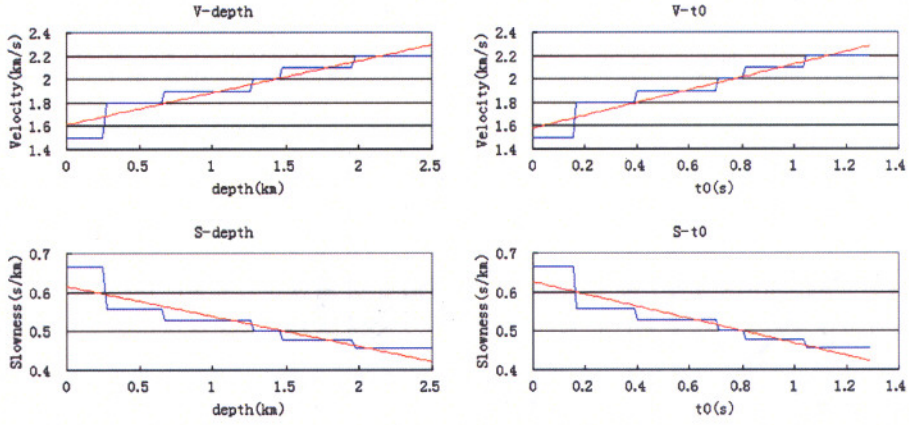

Figure 2. Velocity and slowness of model A (small velocity variations). The blue and red lines represent initial and estimated velocities and slowness respectively. Graphs show velocity variation with depth (top left) and vertical travel time (top right), and slowness variation with depth (bottom left) and vertical travel time (bottom right).

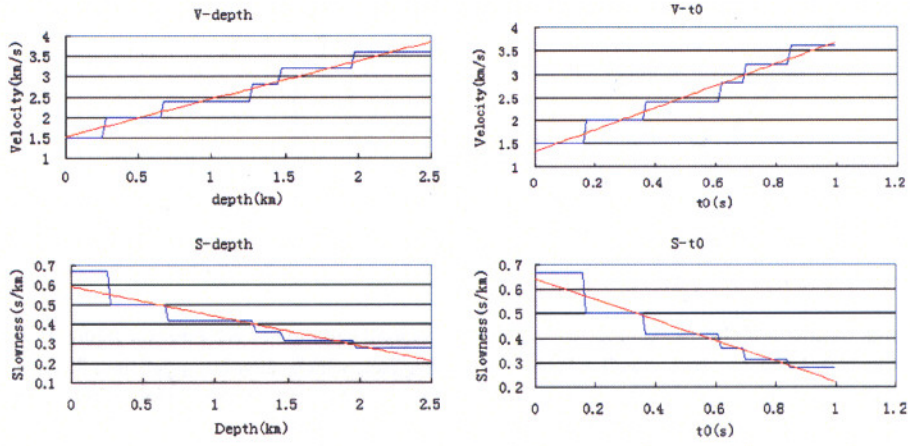

Figure 3. Velocity and slowness of model B (large velocity variations). The blue and red lines represent initial and estimated velocities and slowness respectively. The order and annotation of the graphs are the same as in figure 2.

Considering the travel time curves in figure 5, and the corresponding residuals in figure 7, it is clear that the Taner and Koehler approximation (equation (1)) matches the exact travel time curve very well at small offsets. This must be less than 3 km in the case of model C with a high-velocity layer (see figure 7). However the fit is poor at large offsets, except when the velocity contrasts are small. The approximation can be improved at small offsets by using more terms of the series, but the high powers of offset in the series make it diverge rapidly with increasing offset (Al-Chalabi 1973). Causse *et al* (2000) note that in the presence of a high-velocity layer, the hyperbolic approximation gives relatively large travel time errors even for offsets approximately equal to the reflector depth.

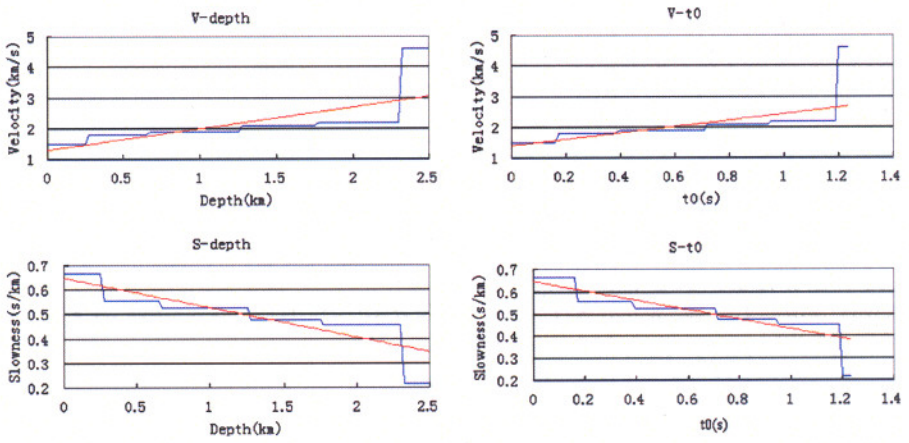

Figure 4. Velocity and slowness of model C (high-velocity layer, where this layer has been moved from the middle to the bottom of the sequence). The order and annotation of the graphs are the same as in figure 2.

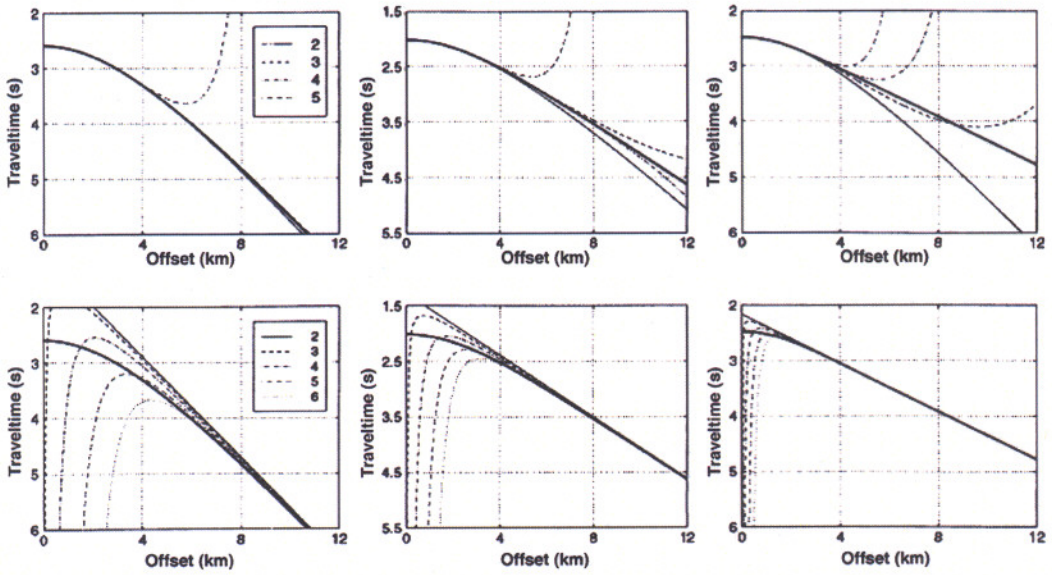

Figure 5. Travel time curves for model A (small velocity variations) on the left, model B (large velocity variations) at the centre and model C (high-velocity layer) on the right. Upper diagrams: Taner and Koehler (1969) approximation. Lower diagrams: Causse *et al* (2000) large-offset approximation. The legend indicates the number of terms used in the respective series. The thick solid line represents the exact travel times curve (Causse *et al* 2000).

Considering the same figures 5 and 7 the Causse series (equation (2)) fits the exact travel time curve very well at large offsets, especially for models containing a high-velocity layer. Approaching zero-offset, the approximate travel times tend to infinity because of the negative powers of offset in the series, when more than two terms are included. Using more terms of the series improves the approximation at large offsets, but makes it diverge slightly more rapidly when approaching near offset. Figure 10 shows the travel times and residual errors for the Causse large-offset approximation for a model with two high-velocity layers, with the interval velocity and depth given in table 2. The Causse approximation shows relatively poor accuracy at small offset for the two examples with no high-velocity layer, especially model A in table 1 where there is only a small variation of velocity (see figure 7). It is accurate at large offset, which must be larger than 3.5 km in the case of model C and 4 km for the model with two high-velocity layers.

In contrast, comparing figures 5–8, the travel times calculated from the equivalent velocity and slowness method are seen to fit the exact travel time curves better than both the Causse and Taner and Koehler approximations along all offsets. Figure 11 shows travel times and residuals calculated by this method for the model with two high-velocity layers. Considering figures 8 and 11 it is seen that the approximation using slowness variation with depth shows relatively high accuracy when used for models with a high-velocity layer (yellow line in figures 9 and 11).

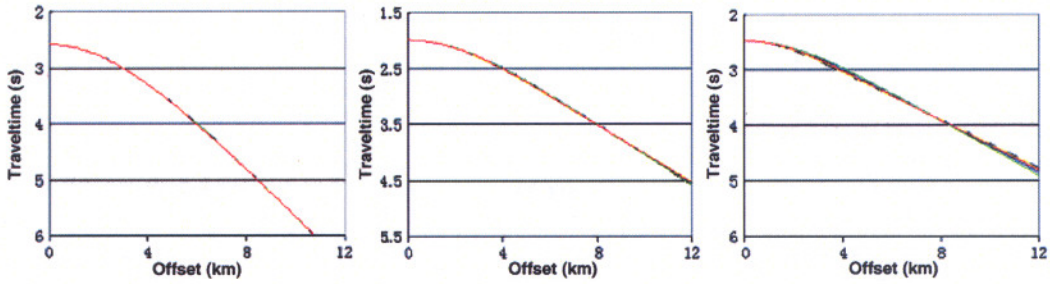

Figure 6. Travel time curves using equivalent functions for model A (small velocity variations) on the left, model B (large velocity variations) at the centre and model C (high-velocity layer) on the right. The black, blue, yellow, green and red lines represent the exact travel time curve, and the curves calculated from functions of velocity with depth, slowness with depth, velocity with vertical travel time and slowness with vertical travel time, respectively.

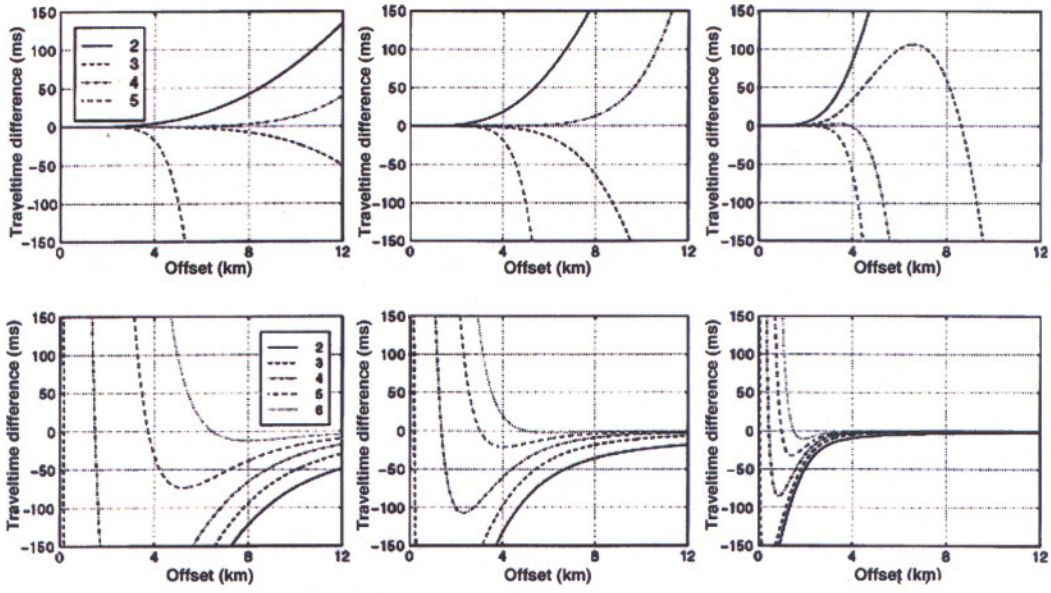

Figure 7. Travel time residuals for models A (small velocity variations) on left, model B (large velocity variations) at centre, and model C (high-velocity layer) on right. Upper diagrams: Taner and Koehler (1969) approximation. Lower diagrams: Causse *et al* (2000) large-offset approximation. The legend indicates the number of terms used in the respective series (Causse *et al* 2000).

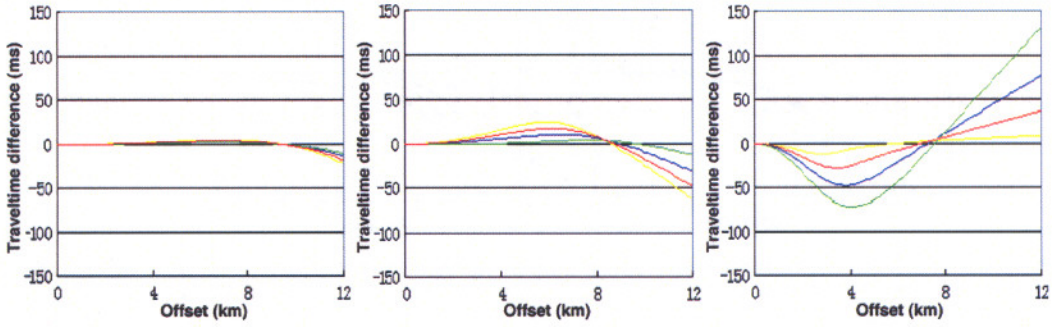

Figure 8. Travel time residuals using equivalent functions for model A (small velocity variations) on the left, model B (large velocity variations) at the centre and model C (high-velocity layer) on the right. The blue, yellow, green and red lines represent the travel time residuals calculated from functions of velocity with depth, slowness with depth, velocity with vertical travel time and slowness with vertical travel time, respectively.

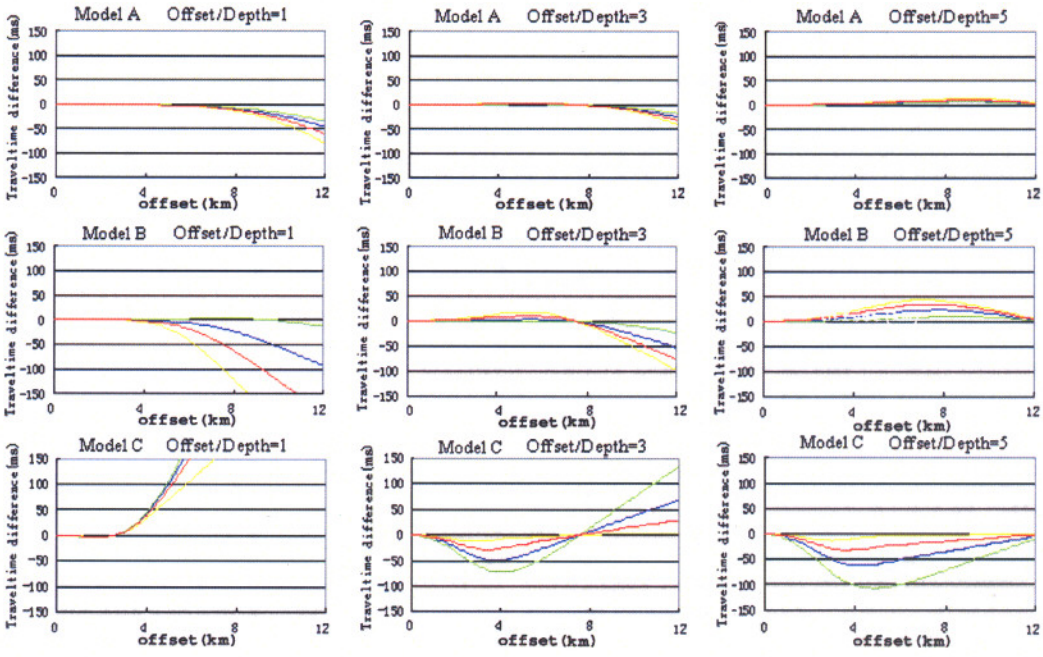

Figure 9. Travel time residuals using equivalent functions for model A (small velocity variations, top), model B (large velocity variations, middle) and model C (high-velocity layer, below). The left, centre and right graphs correspond to offset-to-depth ratios of 1, 3 and 5, respectively. The blue, yellow, green and red lines represent the travel time residuals calculated from functions of velocity with depth, slowness with depth, velocity with vertical travel time and slowness with vertical travel time, respectively.

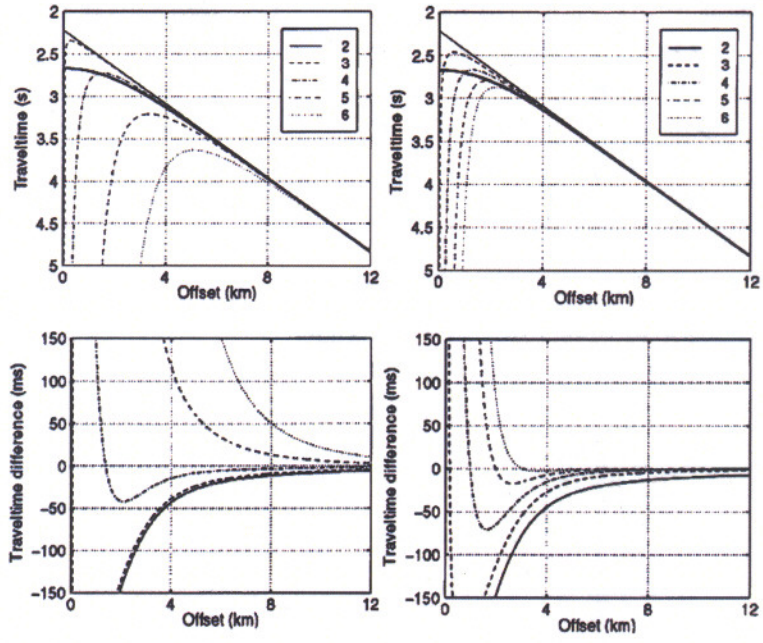

Figure 10. Travel times (top) and travel time residuals (bottom) for the model with two high-velocity layers. The legend indicates the number of terms used in the Causse long-offset travel time series. The coefficients of the series have been calculated by the numbers in table 2 (left curves) and by assuming that both high-velocity layers had a same average velocity of 4599.5 m s^{-1} (right curves). The thick solid line represents the exact travel time curve (Causse *et al* 2000).

To compare the different approximations, figure 12 shows four velocity curves with depth. The curves show the same maximum velocities, but different minimum velocities and variations. The linear velocity variation with depth has constant slope at all depths (blue curve in figure 12). The velocity variation with vertical travel time varies rapidly

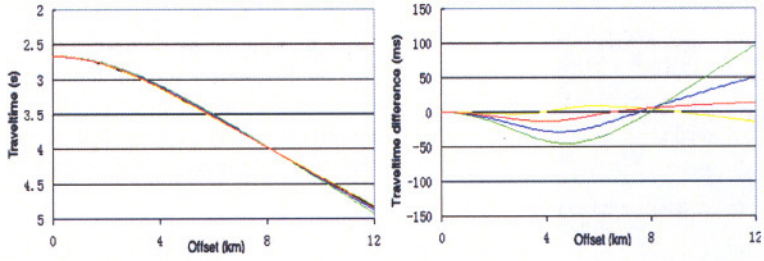

Figure 11. Travel times and travel time residuals for the model with two high-velocity layers. The blue, yellow, green and red lines represent the travel time residuals calculated from functions of velocity with depth, slowness with depth, velocity with vertical travel time and slowness with vertical travel time, respectively.

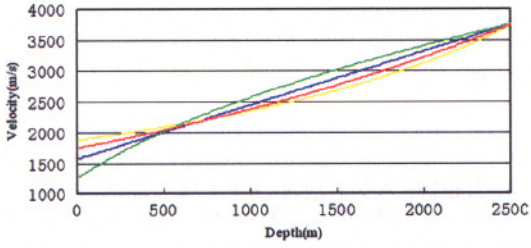

Figure 12. Velocity curves from approximations given by equations (4), (15), (21) and (28). The blue, green, yellow and red lines represent functions of velocity with depth, vertical travel time, slowness with depth and vertical travel time, respectively.

in low-velocity layers (green curve in figure 12). This approximation matches model B (table 1) better than the other three approximations (figure 9 and table 3). The slowness variations with vertical time and depth vary most rapidly in large velocity layers (red and yellow curves in figure 12) among all the approximations. Thus these approximations show the highest accuracy in the model with the high-velocity layer (figures 9, 11 and table 3).

It is appropriate to set out the relations between velocity and slowness variation with depth and vertical travel time. The relation of vertical depth z and vertical travel time t_0 can be written as

$$z = \int_{t_0} V_{t_0}\,\mathrm{d}t_0 = \int_{t_0} \frac{1}{S_{t_0}}\,\mathrm{d}t_0, \tag{38}$$

and

$$t_0 = \int_z \frac{1}{V_z}\,\mathrm{d}z = \int_z S_z\,\mathrm{d}z. \tag{39}$$

Applying equations (38) and (39) to equations (8), (15), (21) and (28), we have

$$\left.\begin{array}{lcl} V_z = V_0 + kz & \Leftrightarrow & V_{t_0} = V_0\exp(kt_0) \\ V_{t_0} = V_0 + \gamma t_0 & \Leftrightarrow & V_z^2 = V_0^2 + 2\gamma z \\ S_z = S_0 + \alpha z & \Leftrightarrow & S_{t_0}^2 = S_0^2 + 2\alpha t_0 \\ S_{t_0} = S_0 + \beta t_0 & \Leftrightarrow & S_z = S_0\exp(\beta z) \end{array}\right]. \tag{40}$$

For calculating travel times, we use the functions of velocity and slowness with depth. For seismic data velocity analysis, it is more convenient to apply the functions of velocity and slowness with vertical travel time.

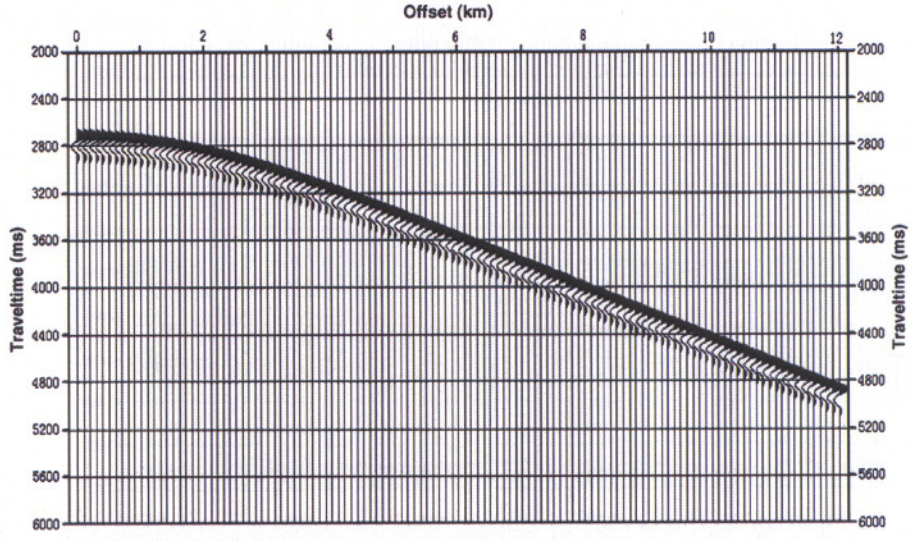

Figure 13. Synthetic CDP records for the model with two high-velocity layers (table 2).

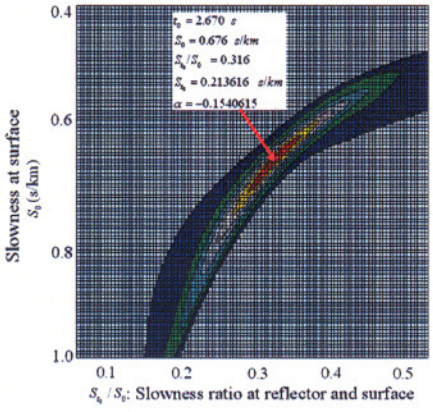

Figure 14. Two-parameter slowness analysis for the synthetic records shown in figure 13. The value of t_0 is read from figure 13 and used in the slowness analysis. The values of S_0 and S_0/S_{t_0} are obtained from the contour plot and used to calculate S_{t_0} and α.

To illustrate the application of the equivalent velocity and slowness approximations to velocity analysis, we take the model with two high-velocity layers (table 2) as an example. The bottom reflector synthetic CDP records are shown in figure 13. A total of 121 receivers at 100 m intervals are used. The minimum and maximum offsets are zero and 12 km, respectively. At reflector depth, velocity V_z and V_{t_0} are the same, and so are S_z and S_{t_0}. Since t_0 can be read from seismic records, we normally use the approximations giving velocity and slowness as a function of t_0. From figure 13, t_0 is approximately 2670 ms. According to the test result, we chose S_0 from 0.4 to 1 s km^{-1} and the ratio of slowness (S_{t_0}/S_0) at the reflector and the surface from 0.1 to 0.5. The parameters $S_z(S_{t_0})$ and α in equation (21) can be calculated through equation (27) from t_0, S_0 and the ratio of slowness. For each pair of S_0 and α, travel times were computed for all offsets.

Figure 14 is the two-parameter slowness semblance analysis for the synthetic records shown in figure 13, in which, the strongest stacking energy is shown in red. The optimum S_0 and ratio of slowness were picked, and S_{t_0} (the slowness at reflector) and α (the slowness gradient) were calculated as 0.213 616 s km^{-1} and –0.154 0615 s km^{-2}. Applying the parameters in equations (25) and (26), we obtained the NMO times. The CDP records with NMO applied are shown in figure 15 at the same scale as figure 13, and also at large scale.

Figure 16 shows the two-parameter velocity analysis method used in real data, in which, the maximum offset is at 7008 m. The two-way vertical travel time from typical reflector is about 1950 ms. Real CMP gather of seismic records is shown in (*a*), the records shown in (*b*) and (*c*) are NMO results using traditional single velocity and two-parameter velocity semblance analysis respectively. We can see that the two-parameter velocity function produces relatively higher accuracy at far offset. These synthetic and real results confirm that the two-parameter approximations are sufficiently accurate for moveout correction of seismic data from near to far offsets.

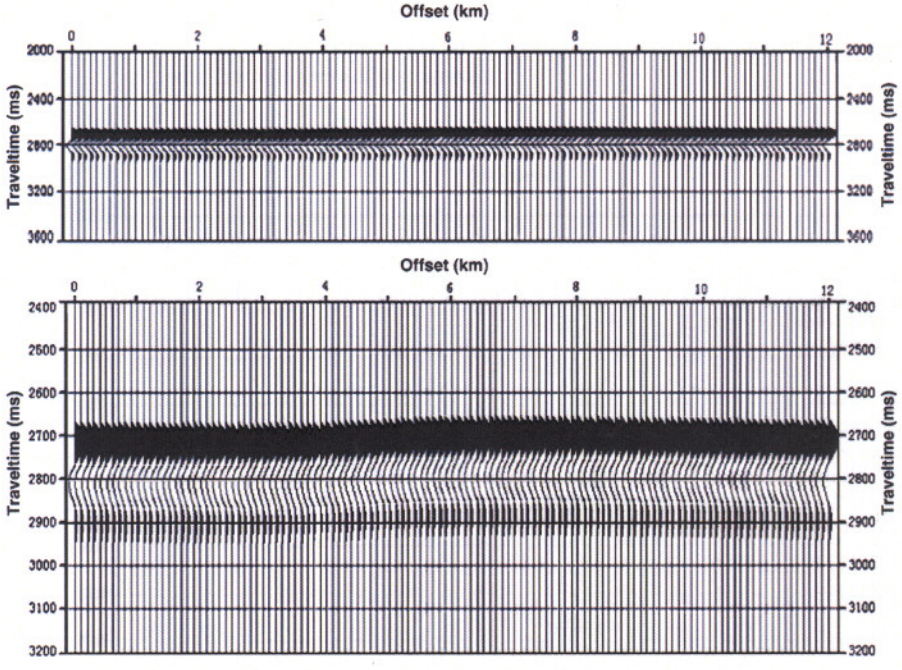

Figure 15. The NMO results of the records in figure 13 following application of the results of two-parameter slowness analysis from figure 14. The profile is shown at the same scale as figure 13 (top), and at a larger scale (below).

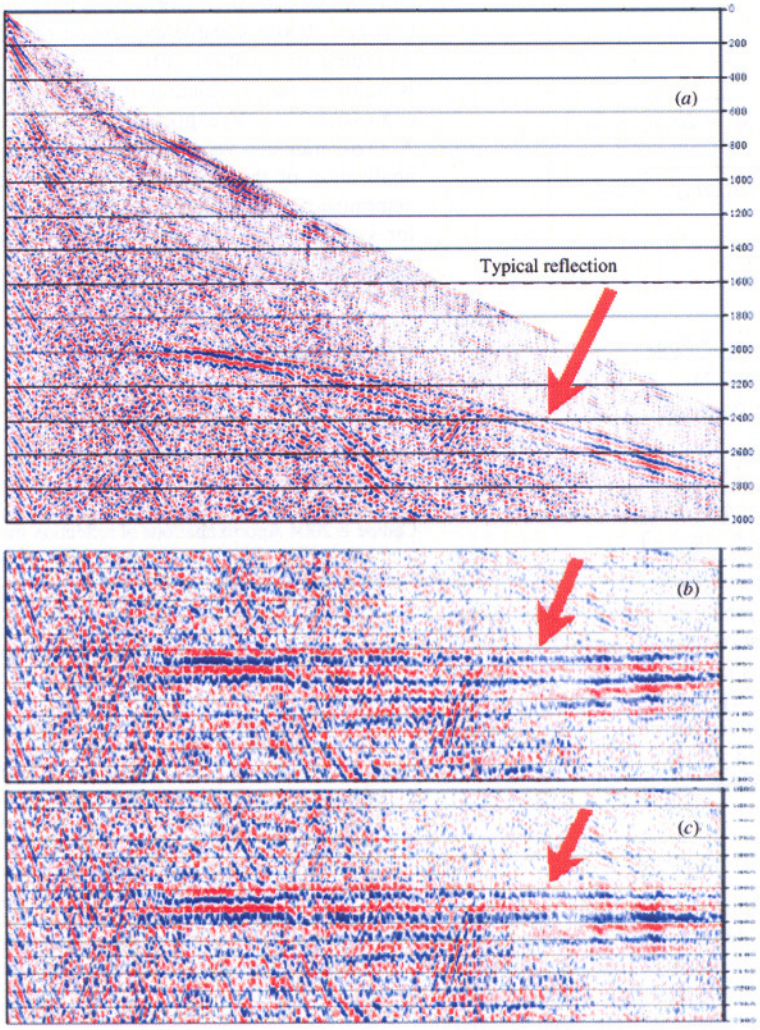

Figure 16. (*a*) Real CMP gather of seismic records, (*b*) and (*c*) are NMO results using traditional single velocity and two-parameter velocity semblance analysis respectively. Maximum offset is at 7008 m. The two-way vertical travel time from typical reflector is about 1950 ms. At far offset, the two-parameter velocity function produces relatively higher accuracy.

The parameters derived from semblance analysis can be used to estimate the velocity model. Considering the relationships in equation (40), we can derive the layer depth z_i, thickness h_i and interval velocity V_i.

For the four different approximations, we have the following expressions.

Velocity variation with depth:

$$z_i = \frac{V_{0,i}[\exp(k_i t_{0,i}) - 1]}{k_i},$$

$$h_i = z_i - z_{i-1} = \frac{V_{0,i}(\exp(k_i t_{0,i}) - 1)}{k_i} - \frac{V_{0,i-1}(\exp(k_{i-1} t_{0,i-1}) - 1)}{k_{i-1}},$$

$$V_i = \frac{h_i}{t_{0,i} - t_{0,i-1}} = \frac{1}{t_{0,i} - t_{0,i-1}}\left[\frac{V_{0,i}(\exp(k_i t_{0,i}) - 1)}{k_i} - \frac{V_{0,i-1}(\exp(k_{i-1} t_{0,i-1}) - 1)}{k_{i-1}}\right]. \quad (41)$$

Velocity variation with vertical travel time:

$$z_i = V_{0,i} t_{0,i} + \frac{1}{2}\gamma_i t_{0,i}^2,$$

$$h_i = z_i - z_{i-1} = (V_{0,i} t_{0,i} - V_{0,i-1} t_{0,i-1}) + \frac{1}{2}\left(\gamma_i t_{0,i}^2 - \gamma_{i-1} t_{0,i-1}^2\right),$$

$$V_i = \frac{h_i}{t_{0,i} - t_{0,i-1}} = \frac{1}{t_{0,i} - t_{0,i-1}}\left[(V_{0,i} t_{0,i} - V_{0,i-1} t_{0,i-1}) + \frac{1}{2}\left(\gamma_i t_{0,i}^2 - \gamma_{i-1} t_{0,i-1}^2\right)\right]. \quad (42)$$

Slowness variation with depth:

$$z_i = \frac{1}{\alpha_i}\left(\sqrt{S_{0,i}^2 + 2\alpha_i t_{0,i}} - S_{0,i}\right),$$

$$h_i = z_i - z_{i-1} = \frac{1}{\alpha_i}\left(\sqrt{S_{0,i}^2 + 2\alpha_i t_{0,i}} - S_{0,i}\right)$$

$$- \frac{1}{\alpha_{i-1}}\left(\sqrt{S_{0,i-1}^2 + 2\alpha_{i-1}t_{0,i-1}} - S_{0,i-1}\right),$$

$$V_i = \frac{h_i}{t_{0,i} - t_{0,i-1}}$$

$$= \frac{1}{t_{0,i} - t_{0,i-1}}\left[\frac{1}{\alpha_i}\left(\sqrt{S_{0,i}^2 + 2\alpha_i t_{0,i}} - S_{0,i}\right)\right.$$

$$\left. - \frac{1}{\alpha_{i-1}}\left(\sqrt{S_{0,i-1}^2 + 2\alpha_{i-1}t_{0,i-1}} - S_{0,i-1}\right)\right]. \quad (43)$$

Slowness variation with vertical travel time:

$$z_i = \frac{1}{\beta_i}\log\frac{S_{0,i} + \beta_i t_{0,i}}{S_{0,i}},$$

$$h_i = z_i - z_{i-1} = \frac{1}{\beta_i}\log\frac{S_{0,i} + \beta_i t_{0,i}}{S_{0,i}}$$

$$- \frac{1}{\beta_{i-1}}\log\frac{S_{0,i-1} + \beta_{i-1}t_{0,i-1}}{S_{0,i-1}},$$

$$V_i = \frac{h_i}{t_{0,i} - t_{0,i-1}} = \frac{1}{t_{0,i} - t_{0,i-1}}\left[\frac{1}{\beta_i}\log\frac{S_{0,i} + \beta_i t_{0,i}}{S_{0,i}}\right.$$

$$\left. - \frac{1}{\beta_{i-1}}\log\frac{S_{0,i-1} + \beta_{i-1}t_{0,i-1}}{S_{0,i-1}}\right]. \quad (44)$$

In the presence of anisotropy produced by thin-layered media, the two-parameter approximations can be used to get highly accurate results. Since in this case the anisotropy is caused by a vertical variation of velocity, the methods described here are well matched to the situation. However, in the presence of azimuthal anisotropy, a third parameter will be required to estimate seismic wave travel times.

Conclusions

We have extended the approximation of seismic travel times using velocity variation with depth to approximations based on velocity variation with vertical travel time, and slowness variation with depth and vertical travel time. Solutions for all four types of velocity or slowness have been derived. The new method was compared with the approximations of Taner and Koehler (1969) and Causse *et al* (2000) for plane-layered isotropic media. It provides a much better match to exact travel times at all offsets, even though the functions only consist of two terms. The function which uses the slowness variation with depth works particularly well in the presence of a thin high-velocity layer and with two high-velocity layers. The relationships between velocity and/or slowness with depth and/or vertical travel time were discussed. One can choose suitable expression of velocity or slowness according to equation (40). For example, $V_z = V_0 + kz$ is suitable for calculating travel times but its equivalent expression $V_{t_0} = V_0 \exp(kt_0)$ is better for semblance analysis. A two-parameter velocity/slowness analysis illustrated the application of the functions. Optimum parameters can be determined from semblance analysis. The results of NMO for synthetic and real seismic records show that the two-parameter approximations produce relatively high accuracy for all offsets.

References

Al-Chalabi M 1973 Series approximation in velocity and traveltime computations *Geophys. Prospect.* **21** 783–95

Al-Chalabi M 1974 An analysis of stacking, rms, average, and interval velocities over a horizontally layered ground *Geophys. Prospect.* **22** 458–75

Causse E 2004 Approximations of reflection travel times with high accuracy at all offsets *J. Geophys. Eng.* **1** 28–45

Causse E, Haugen G U and Rommel B E 2000 Large-offset approximation to seismic reflection traveltimes *Geophys. Prospect.* **48** 763–78

Causse E and Sénéchal P 2006 Model-based automatic dense velocity analysis of GPR field data for the estimation of soil properties *J. Geophys. Eng.* **3** 169–76

Dix C X 1955 Seismic velocities from surface measurements *Geophysics* **20** 68–86

Gidlow P M and Fatti J L 1990 Preserving far offset seismic data using non-hyperbolic moveout correction *60th SEG Meeting (San Francisco, USA)* pp 1726–9 (Expanded Abstracts)

Hake H, Helbig K and Mesdag C S 1984 Three-term Taylor series for t22×2-curves of P- and S-waves over layered transversely isotropic ground *Geophys. Prospect.* **32** 828–50

Kaila K L and Sain K 1994 Errors in RMS velocity and zero-offset two-way time as determined from wide-angle seismic reflection traveltimes using truncated series *J. Seismic Explor.* **3** 173–88

May B T and Straley D K 1979 Higher-order velocity spectra *Geophysics* **44** 1193–207

Taner M T and Koehler F 1969 Velocity spectra—digital computer derivation and application of velocity functions *Geophysics* **34** 859–81

Thore P, de Bazelaire E and Ray M 1994 The three-parameter equation: an efficient tool to enhance the stack *Geophysics* **59** 297–308

Tsvankin I and Thomsen L 1994 Non-hyperbolic reflection moveout in anisotropic media *Geophysics* **59** 1290–304